of bleeding episodes and of the use of FVIII concentrates. Data on clinical trials of hemophilia A gene therapy support this notion.[12] However, this human FVIII level in mouse plasma was lower than that expected from the observed *in vitro* production rate. One contributing factor may be the shorter half-life of human FVIII in mice compared to humans. The half-life of injected human FVIII in mice is approximately 1 h,[13] whereas the half-life in hemophilia patients is closer to 8–12 h. Another possibility may be the inefficient transduction of adipocytes *in vivo* because the vector-containing solution might not diffuse throughout the adipose tissues, resulting in less adipocytes being exposed to the viral vectors. It is also possible that transduction of mouse adipocytes by the SIV vector is less efficient than that of human cells. Production of human FVIII from differentiated 3T3-L1 cells, transduced with the SIVhFVIII vector, was significantly lower than that from human adipocytes (not shown). The observation that anti-human FVIII antibodies were present in the mouse plasma obtained on day 14 and subsequently increased to 6.9 μg/ml by day 25 suggested that human FVIII was rapidly cleared from the mouse circulation by the formation of immune complexes after day 14. Thus, human FVIII was secreted into the circulation and was recognized by the *db/db* mouse immune system. The notion that human FVIII was synthesized in the adipocyts *in vivo* is also supported by detection of human FVIII gene transcripts and products in the adipocytes. In conclusion, adipose tissue is easily accessible and is an appropriate target for gene delivery. Recombinant SIV vectors may be applicable for adipocyte-targeted gene therapy for hemophilia A.

Materials and methods

Cell culture

Human white adipocytes prepared in 24-well culture plates were purchased from Zen-Bio Inc. (Research Triangle Park, NC, USA). These cells were differentiated from preadipocytes isolated from the adipose tissue of 49-year-old healthy subjects undergoing liposuction surgery with informed consent. The cells were shown to express leptin, CCAAT/enhancer-binding protein α, peroxisome proliferator-activated receptor γ, and STATs.[14,15] Human adipocytes were cultured in DMEM/HAM F10 medium supplemented with 3% fetal bovine serum, 15 mM HEPES, biotin (33 μM), pantothenate (17 μM), insulin (100 nM), dexamethazone (1 μM), penicillin 100 U/ml, streptomycin (100 μg/ml), and amphotericin B (0.25 μg/ml) (Zen-Bio Inc.). 3T3-L1 cells (ATCC) were cultivated in DMEM containing 10% FBS. Differentiation of 3T3-L1 cells to adipocytes was carried out in the medium containing dexamethasone, insulin, and 1-methyl-3 isobutylxantine, as described previously.[16]

Production of SIVagm vectors

Human FVIII cDNA spanning the entire coding region was a generous gift from Dr JA van Mourik (VU University Medical Centre).[17] As the B domain is excised from other FVIII domains upon activation by thrombin and is not essential for coagulation activity of FVIIIa, coding for the B domain was deleted from the human FVIII cDNA by PCR-based mutagenesis (BDD FVIII cDNA), as described previously.[18] The deletion was confirmed by sequencing. The characteristics and production of SIVagm vector used in this study were described previously.[19] Self-inactivating SIVagm vectors are pseudotyped with vesicular stomatitis virus glycoprotein G (VSVG). We constructed a series of gene transfer vectors to express the eGFP gene, the lacZ gene, and the hBDDFVIII gene driven by the cytomegalovirus (CMV) promoter. To produce SIV vectors, 293T cells were transfected with the packaging vector, the gene transfer vector, and pVSVG (Clontech), as described previously.[19] Transduction units of SIVeGFP were determined by infection of SIVeGFP to 293T cells, followed by determination of eGFP expression by FACS analysis. RNA dot blot analysis was performed to quantify the amount of SIVagmTYO1vector genome of vector preparations. When SIVhFVIII was produced in 293T cells, SIVeGFP also was prepared simultaneously and the transduction unit of SIVeGFP and the amount of vector genome were determined. The SIVeGFP preparation was used as the standard to estimate the transduction units of SIVhFVIII.

In vitro culture and transduction of human adipocytes

For transduction, increasing concentrations of the SIV vector were added to human adipocyte cell monolayers in 24-well culture plates, and the cells were incubated at 37°C for 48 h in the presence of 5% CO_2. After incubation, the medium was harvested and changed, according to the manufacturer's instruction. SIVeGFP-transduced adipocytes were analyzed for eGFP expression by fluorescence microscopy and flow cytometry, and the conditioned medium of SIVhFVIII-transduced adipocytes was harvested and subjected to FVIII ELISA. To study the secretion of FVIII from adipocytes transduced with SIVhFVIII, pulse-chase experiments were performed. SIVhFVIII-transduced adipocytes were cultured for 30 min in methionine-deficient DMEM (GIBCO-Invitrogen Japan, Tokyo, Japan) containing 3700 kBq/ml [^{35}S]-methionine (NEN Life Science Products, Inc., Boston, MA, USA), and then cultured in the complete medium (DMEM). After various incubation time periods, conditioned medium and cell extracts were prepared. To isolate [^{35}S]-labeled FVIII molecules, the conditioned media and cell lysates were subjected to immunoprecipitation using sheep polyclonal antibodies against human FVIII and protein A-coupled Sepharose CL-4B (Amersham Pharmacia Biotech, UK). [^{35}S]-labeled FVIII was analyzed by SDS-PAGE followed by autoradiography, and quantified using an image analyzer BAS 2000 (Fujifilm, Tokyo, Japan), as described.[20]

Mice

Experimental *db/db* mice (C57BL/KsJ-db/db) are well characterized obese and diabetic mice caused by the genetic abnormality of the leptin receptor gene,[21] and were purchased from Japan SLC Inc. (Hamamatsu, Japan). The *db/db* mice were kept in a clean P3-level experimental room, and were maintained on a sterile diet and given autoclaved water.

Transduction of mouse adipose tissues by SIV vectors

SIV vectors carrying either the lacZ gene or the hFVIII gene were diluted in PBS and injected into the subcutaneous adipose tissue of the mice. Peripheral

blood (100 µl) was collected from mouse tail veins into tubes containing heparin. Platelet poor plasma was prepared by centrifugation of the peripheral blood at 1000 g for 15 min, and subjected to FVIII ELISA. Some mice were killed on day 14 after the injection for detection of transcripts and products of the transgenes.

Enzyme immunosorbent assay (ELISA) for human FVIII antigen

Since human FVIII clotting activity could not be quantified directly in the *db/db* mice because of the presence of endogenous murine FVIII, human FVIII expressed in *db/db* mice was quantified by a human FVIII-specific ELISA, as described previously.[22] Briefly, 96-well microtiter plates (Costar, Cambridge, MA, USA) were coated with 1 µg/ml mouse monoclonal antibody to human FVIII (Chemo-Sero Institute, Kumamoto, Japan). After blocking with 5% casein in PBS, mouse plasma samples or pooled normal human plasma in Tris-buffered saline (TBS) containing 0.1% Tween 20, 1% casein were added. After 16 h incubation at 4°C, human FVIII bound to the plates was detected with sheep anti-human FVIII polyclonal antibodies (Cedarlane Laboratories Ltd, Homby, Ontario, Canada) and horseradish peroxidase-conjugated rabbit anti-sheep IgG.

Detection of anti-human FVIII mouse antibody

Microtiter plates were coated with purified human FVIII in PBS for 16 h. After blocking with 5% casein, FVIII-coated microtiter plates were incubated with mouse plasma at 10–1000-fold dilutions or monoclonal antibodies raised against human FVIII as the standard. Mouse IgG bound to human FVIII was detected by HRP-conjugated anti-mouse IgG, followed by incubation with HRP substrate ABTS (Kirkegaard & Perry Laboratories, Inc., Gaithersburg, MD, USA).

Detection of β-galactosidase and human FVIII in the mouse adipose tissue

Mouse adipose tissues were obtained from *db/db* mice. The adipose tissues were fixed with 2% paraformaldehyde in PBS for 5 min, washed with PBS, and then incubated in PBS containing 1 mg/ml X-gal, 2 mM $MgCl_2$, 5 mM $K_4Fe(CN)_6$, 5 mM $K_3Fe(CN)_6$, 0.01% Na deoxycholate, 0.1% Triton X-100 for 1 h. The tissues were again washed, incubated with PBS containing sucrose (10–30%), and frozen with OTC compound (Tissue-Tek, Miles Inc., Elkhart, IN, USA) in dry ice/ethanol. Tissue sections were made at −35°C and attached to poly-lysine-coated glass slides. For the immunofluorescence study, the adipose tissues were fixed with 4% paraformaldehyde in PBS for 2 h at 4°C, incubated with PBS containing sucrose (10–30%), and then frozen in the presence of OCT compound in dry ice/ethanol. Sections were prepared from frozen tissues at −35°C and attached to polylysine-coated glass slides. For the detection of human FVIII, tissue sections were blocked with 1% bovine serum albumin in PBS. Samples were incubated with polyclonal anti-human FVIII antibody at 4°C for 16 h. After washing in PBS, cells were incubated with donkey anti-sheep IgG antibody conjugated with Alexa488 (Molecular Probes, Eugene, OR, USA) at 4°C for 16 h for visualization of human FVIII by fluorescence microscopy.

Detection of the BDD-FVIII transcript by RT-PCR

RNA was isolated from the adipose tissue by the acid-guanidine method and was reverse transcribed to cDNA using reverse transcriptase (Superscript, Invitrogen Japan, Tokyo, Japan) and oligo-(dT) primers in a 20 µl mixture (QIAGEN Japan, Tokyo, Japan) after DNase I (Amplification grade, Invitrogen) treatment. Subsequent PCR amplification was carried out with 1 µl of cDNA solution in a 50 µl reaction mixture containing 5 U of Taq polymerase, 10 mmol/l Tris-HCl (pH 8.5), 50 mM KCl, 1.5 mM $MgCl_2$, and 100 µM dNTPs in the presence of specific primer pairs (200 nM) designed to amplify the DNA fragments derived from the transcript of the BDD-FVIII transgene. Each PCR cycle consisted of denaturation at 94°C for 15 s, annealing at 55°C for 30 s, and extension at 72°C for 30 s. The PCR products were analyzed by agarose gel electrophoresis. Authenticity of PCR products was confirmed by their molecular sizes after agarose gel electrophopresis, and by sequencing. The primer sequences for human FVIII are ATTGGAG-CACAGACTGACTT and ATATGGTATCATCATAGTCA (400 bp). Primers for mouse GAPDH were purchased from R&D Systems, Inc. (Minneapolis, MN, USA).

Acknowledgements

We thank Dr JA van Mourik for the full-length FVIII cDNA and Dr Nakagaki (Chemo Sero Institute) for monoclonal antibodies to human FVIII. We also thank Dr DJ Stearns-Kurosawa (IdEst, Inc) for critical reading and editing of this manuscript, and Ms Fumino Muroi for technical assistance. This work is supported by Grants-in-aid for Scientific Research #12670687 to JM and #13671078 to SM from the Ministry of Education and Science, and by Health and Labour Sciences Research Grants for Research on HIV/AIDS to KO and to YS from the Ministry of Health, Labour and Welfare.

References

1 Hoyer LW. Hemophilia A. *N Engl J Med* 1994; **330**: 38–47.
2 Kay MA, High K. Gene therapy for the hemophilias. *Proc Natl Acad Sci USA* 1999; **96**: 9973–9975.
3 Mohamed-Ali V, Pinkney JH, Coppack SW. Adipose tissue as an endocrine and paracrine organ. *Int J Obes Relat Metab Disord* 1998; **22**: 1145–1158.
4 Kaufman RJ, Wasley LC, Dorner AJ. Synthesis, processing, and secretion of recombinant human factor VIII expressed in mammalian cells. *J Biol Chem* 1988: 6352–6362.
5 Levine JA, Eberhardt NL, Jensen MD, O'Brien T. Adenoviral-mediated gene transfer to human adipocytes *in vitro*, and human adipose tissue *ex vivo* and rabbit femoral adipose tissue *in vivo*. *J Nutr Sci Vitaminol* 1998; **44**: 569–572.
6 Nagamatsu S *et al*. Adnovirus-medicated proproinsulin gene transfer into adipose tissues ameliorates hyperglycemia in obese diabetic KKA^y mice. *FEBS Lett* 2001; **509**: 106–110.
7 Miyoshi H *et al*. Transduction of human CD34+ cells that mediate long-term engraftment of NOD/SCID mice by HIV vectors. *Science* 1999; **283**: 682–686.
8 Chen W *et al*. Lentiviral vector transduction of hematopoietic stem cells that mediate long-term reconstitution of lethally irradiated mice. *Stem Cells* 2000; **18**: 352–359.
9 Woods NB *et al*. Lentiviral gene transfer into primary and secondary NOD/SCID repopulating cells. *Blood* 2000; **96**: 3725–3733.

10 Naldini L *et al.* *In vivo* gene delivery and stable transduction of nondividing cells by a lentiviral vector. *Science* 1996; **272**: 263–267.
11 Honjo S *et al.* Experimental infection of African green monkeys and cynomolgus monkeys with a SIVAGM strain isolated from a healthy African green monkey. *J Med Primatol* 1990; **19**: 9–20.
12 Roth DA, The factor FIII transkaryotic therapy study group *et al.* Implantation of non-viral *ex vivo* genetically modified autologous dermal fibroblaststhat express B-domain deleted human factor VIII in 12 severe hemophilia A study subjects. *Blood* 2002; **100** (Suppl): 116a (abstract #430).
13 Dwarki VJ *et al.* Gene therapy for hemophilia A: production of therapeutic levels of human factor VIII *in vivo* in mice. *Proc Natl Acad Sci USA* 1995; **14**: 1023–1027.
14 Halvorsen YC *et al.* Thiazolinediones and glucocortidoids synergistically induce differentiation of human adipose tissue stromal cells: biochemical, cellular, and molecular analysis. *Metabolism* 2001; **50**: 407–413.
15 Harp JB, Franklin D, Vanderpuije AA, Gimble JM. Differential expression of signal transducers and activators of transcription during human adipogenesis. *Biochem Biophys Res Commun* 2001; **281**: 907–912.
16 Weiss GH, Rosen OM, Rubin CS. Regulation of fatty acid synthetase concentration and activity during adipocyte differentiation. *J Biol Chem* 1980; **255**: 4751–4757.
17 Mertens K *et al.* Biological activity of recombinant factor VIII variants lacking the central B-domain and the heavy-chain sequence Lys713-Arg740: discordant *in vitro* and *in vivo* activity. *Br J Haematol* 1993; **85**: 133–142.
18 Lind P *et al.* Novel forms of B-domain-deleted recombinant factor VIII molecules. Construction and biochemical characterization. *Eur J Biochem* 1995; **232**: 19–27.
19 Nakajima T *et al.* Development of novel simian immunodeficiency virus vectors carrying a dual gene expression system. *Hum Gene Ther* 2000; **11**: 1863–1874.
20 Naito M *et al.* Defective sorting to secretory vesicles in the trans Golgi network is partly responsible for protein C deficiency: molecular mechanisms of impaired secretion of abnormal protein C R169W, R352W, and G376D. *Circ Res* 2003; **92**: 865–872.
21 Chua Jr S-C *et al.* Phenotypes of mouse diabetes and rat fatty due to mutations in the OB (leptin) receptor. *Science* 1996; **271**: 994–996.
22 Yonemura H *et al.* Efficient production of recombinant human factor VIII by co-expression of the heavy and light chains. *Protein Eng* 1993; **6**: 669–674.

Journal of Thrombosis and Haemostasis, **1**: 2356–2359

ORIGINAL ARTICLE

Hypofibrinogenemia caused by a nonsense mutation in the fibrinogen Bβ chain gene

J. MIMURO, A. HAMANO, T. TANAKA,* K. S. MADOIWA, T. SUGO, M. MATSUDA and Y. SAKATA

*Cell and Molecular Medicine, Center for Molecular Medicine, Jichi Medical School, Tochigi-ken, and *Department of Internal Medicine, Tottori Prefectural Hospital, Tottori-ken, Japan*

To cite this article: Mimuro J, Hamano A, Tanaka T, Madoiwa KS, Sugo T, Matsuda M, Sakata Y. Hypofibrinogenemia caused by a nonsense mutation in the fibrinogen Bβ chain gene. *J Thromb Haemost* 2003; **1**: 2356–9.

Summary. Congenital hypofibrinogenemia, fibrinogen Tottori II, caused by a nonsense mutation in the fibrinogen Bβ chain gene, was found in a 68-year-old Japanese female. The plasma fibrinogen level was 99.2 mg dL^{-1} as determined by the thrombin time method. No overt molecular abnormalities were observed in purified patient fibrinogen by SDS–PAGE analysis. After sequencing all exons and exon–intron boundaries of three fibrinogen genes, we found a heterozygous single point mutation of T→G at position 3356 of the patient fibrinogen Bβ chain gene. This nucleotide mutation results in a nonsense mutation (TAT sequence for Bβ 41Tyr to TAG sequence for a translation termination signal). The mutation was confirmed by polymerase chain reaction-restriction fragment length polymorphism analysis, since this nucleotide mutation results in a new NheI recognition sequence at this position. These data indicated that the nonsense mutation of the fibrinogen Bβ chain gene caused a truncated fibrinogen Bβ chain, which may not be assembled in the fibrinogen molecule.

Keywords: fibrinogen, gene analysis, hypofibrinogenemia.

Introduction

Fibrinogen is a 340-kDa plasma protein that participates in the final step of blood coagulation and also plays an important role in platelet aggregation [1,2]. Thus, a significant decrease in blood fibrinogen levels can lead to a bleeding diathesis. Fibrinogen is composed of two identical molecular halves, each being composed of an Aα, Bβ, and a γ chain. These three polypeptides are encoded by three independent genes, clustered on chromosome 4. During synthesis in the liver, these chains are translated, processed, and assembled to the mature molecules [3]. Many reports have shown that a variety of genetic mutations result in molecular defects in fibrinogen molecules (dysfibrinogen) or decreased levels of fibrinogen in blood (afibrinogenemia and hypofibrinogenemia).

Patients with hereditary hypofibrinogenemia have bleeding tendencies, depending on their plasma level of fibrinogen. Molecular mechanisms of hereditary hypofibrinogenemia may be assigned to nonsense mutations, missense mutations, nucleotide insertions, or nucleotide deletions in one of the fibrinogen genes [4]. Here, we report a new hypofibrinogenemia caused by a nonsense mutation in the fibrinogen Bβ chain gene.

Correspondence: Yoichi Sakata, Cell and Molecular Medicine, Jichi Medical School, Tochigi-ken, 329-0498, Japan.
Tel.: +81 285 58 7397; fax: +81 285 44 7817; e-mail: yoisaka@jichi.ac.jp

Received 19 April 2003, accepted 28 May 2003

Materials and methods

Patient description

A 68-year-old Japanese woman was found to have hypofibrinogenemia upon medical examination for epistaxis. The episode of epistaxis was neither severe nor prolonged. The patient had not been suffering from spontaneous bleeding or thrombosis. No severe bleeding was observed during pregnancy or delivery. No apparent bleeding tendency was found in relatives. Laboratory tests were normal except for the decreased level of plasma fibrinogen and were as follows: bleeding time 1.5 min, prothrombin time (PT) 10.7 s, PT-International Normalized Ratio (INR) 0.89, activated partial thromboplastin time 29.4 s, fibrin degradation product (FDP) <5 μg mL^{-1}, fibrinogen 99.2 mg dL^{-1} (thrombin time method), RBC 486×10^4 μL^{-1}, Hb 14.8 g dL^{-1}, Ht 44.5%, platelet 22.8×10^4 μL^{-1}, WBC 5600 μL^{-1}, AST 16 (8–28) IU L^{-1}, ALT 21 (3–35) IU L^{-1}, alkaline phosphatase 210 (68–220) IU L^{-1}, LDH 158 (170–370) IU L^{-1}, leucine aminopeptidase 54 (75–125) IU L^{-1}, T-bil 1.1 mg dL^{-1}, total protein 7.1 g dL^{-1}, Alb 4.2 g dL^{-1}, BUN 21 mg dL^{-1}, creatinine 0.46 (0.5–0.9) mg dL^{-1}. Based upon these data, the patient did not appear to have liver dysfunction that could develop secondary hypofibrinogenemia or anemia caused by bleeding tendency. Inasmuch as hereditary hypofibrinogenemia was suspected, we conducted molecular and genetic analyses of patient fibrinogen. Subsequent analyses of patient protein and genes were carried out with informed consent.

Analysis of fibrinogen by SDS–PAGE

Fibrinogen was purified from patient plasma as described previously [5] and was analyzed by SDS–PAGE under reducing conditions and was compared with normal fibrinogen. Purified patient fibrinogen was incubated with thrombin in the absence or presence of factor XIII and 2.5 mM Ca^{2+} ions to investigate release of fibrinopeptides A and B and the cross-linking profiles of γ chains (γ dimer formation) and α chains (α polymer formation) as described previously [5].

Determination of the nucleotide sequences of fibrinogen genes

Patient genomic DNA was isolated from peripheral leukocytes by standard procedures as described previously [5]. All exons including exon–intron boundaries of fibrinogen genes were amplified by polymerase chain reaction (PCR) using Bucabest DNA polymerase (Takara Co., Kyoto, Japan). Primers (Invitrogen Japan, Tokyo, Japan) were designed for amplification of each exon, including the exon–intron boundaries of each fibrinogen gene. PCR-amplified DNA fragments were isolated after agarose gel electrophoresis using a rapid gel extraction kit (Invitrogen) and their nucleotide sequences were determined directly by the dideoxynucleotide termination reaction method using BigDye cycle sequencing kit and a DNA sequencer model ABI 310 (Applied Biosystems Inc. Japan, Tokyo, Japan). Some DNA fragments were cloned into the pCR2.1-TOPO plasmid vector using a TOPO TA cloning kit (Invitrogen) and their nucleotide sequences were determined.

Cleavage of PCR-amplified DNA fragments by NheI

DNA fragments from the fibrinogen Bβ chain gene, including exons I, II, III, and IV, together with introns were amplified using EX taq (Roche Diagnostics GmbH, Mannheim, Germany). The amplified DNA fragment, which corresponded to exons I, II, III, and IV, and the DNA fragment which corresponded to exon II of the fibrinogen Bβ chain were treated with NheI and analyzed by agarose gel electrophoresis.

Results

Figure 1 shows the SDS–PAGE analysis of purified fibrinogen. In comparison with normal fibrinogen, there were no apparent molecular weight differences between patient fibrinogen and normal fibrinogen, conversion of Aα and Bβ chains to α and β chains by thrombin, or cross-linking of γ and α chains. The

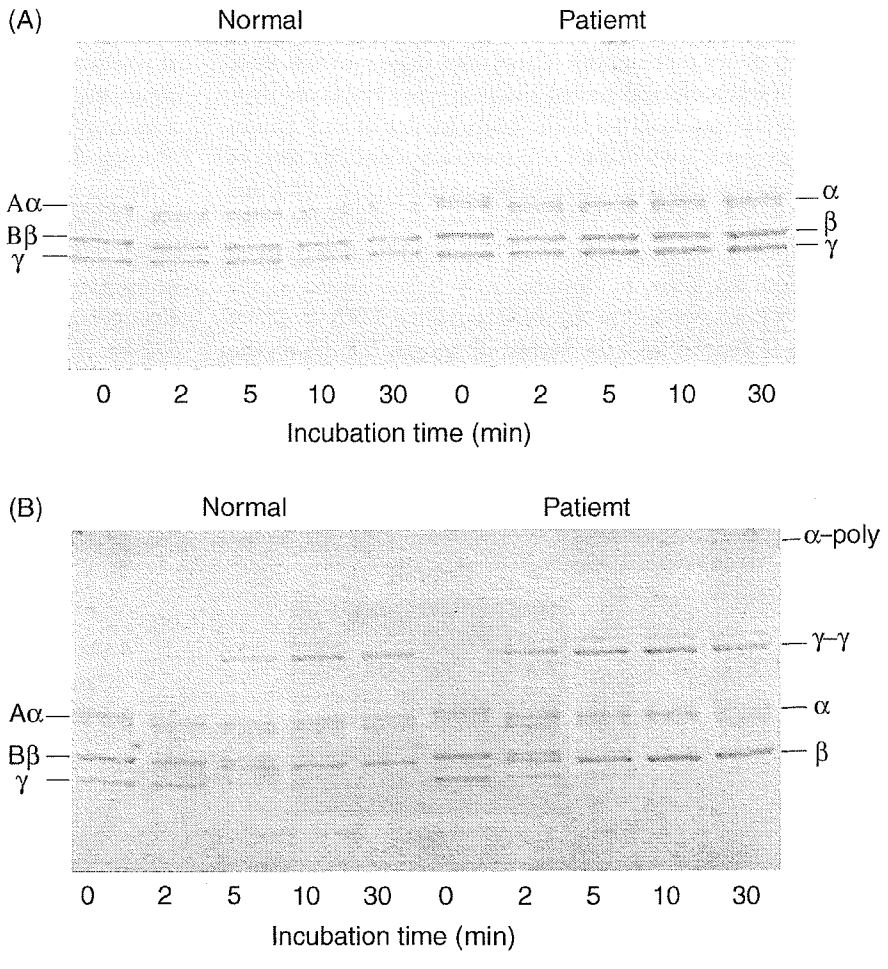

Fig. 1. SDS–PAGE analysis of purified fibrinogen. Fibrinogen was purified from citrated plasma derived from the patient and normal subjects and was studied for the apparent molecular mass, the release of fibrinopeptides A and B by thrombin and cross-linking of γ and α chains. (A) Conversion of Aα and Bβ chains to α and β chains by thrombin treatment in the absence of Ca^{2+} ions. Formation of γ dimer (γ-γ) and α polymer (α-poly) upon thrombin treatment in the presence of factor XIII and 2.5 mM Ca^{2+} was analyzed by SDS–PAGE (B).

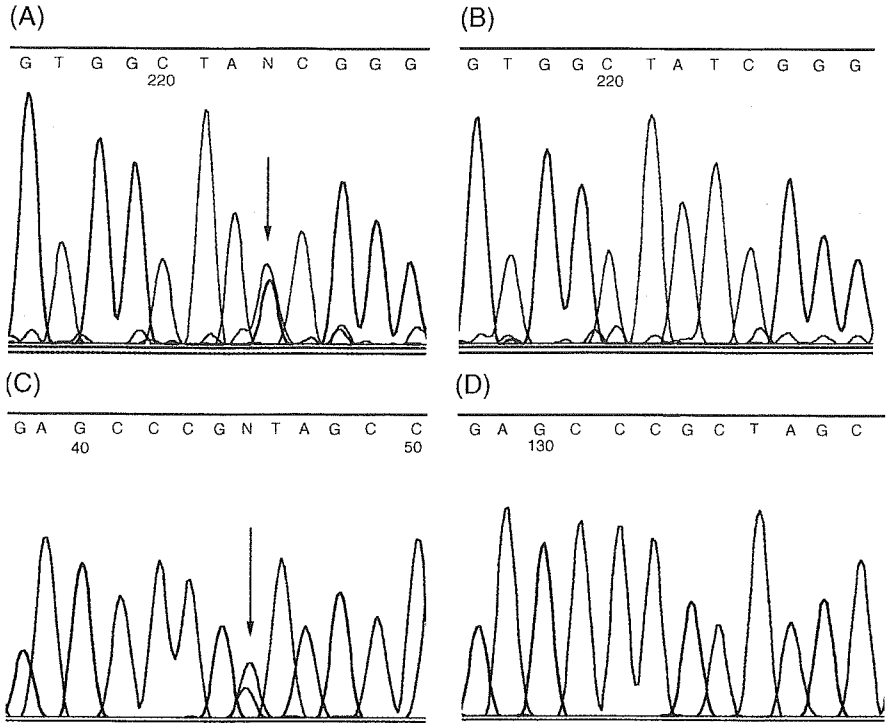

Fig. 2. The nucleotide sequence of exon II of the Bβ chain gene. (A) The nucleotide sequence of polymerase chain reaction-amplified DNA fragments of exon II derived from the patient fibrinogen Bβ chain gene. The arrow indicates position 3356 where both T and G were present. Only T was found at the corresponding position in a normal fibrinogen Bβ chain gene (B). A and C were present at the same position (arrow) of the complementary strand of exon II of the patient fibrinogen Bβ chain gene (C). After cloning the DNA fragment into pCR 2.1 TOPO, the nucleotide sequence of exon II was determined. (D) The sequence of the complementary strand of exon II of the fibrinogen Bβ chain gene. A was identified instead of C at position 3356.

thrombin time of purified Tottori II fibrinogen was 14.2 s (13.4 s) in the absence of Ca^{2+} ions. The polymerization profiles of fibrin monomers derived from patient fibrinogen were not impaired either (not shown). These data suggested that there were no overt molecular abnormalities in major functional sites. After determination of the nucleotide sequence of each patient fibrinogen gene, we found a T→G mutation at position 3356 of the patient fibrinogen Bβ gene. As shown in Fig. 2A, both T and G were found at position 3356 in the directly sequenced PCR-amplified DNA fragments of exon II derived from the patient fibrinogen Bβ gene. In contrast, only T was found at the corresponding position in the PCR-amplified DNA fragment of exon II derived from the normal fibrinogen Bβ chain gene (Fig. 2B). To confirm these data, we sequenced the complementary strand of exon II of the patient fibrinogen Bβ gene and found A and C at this position (Fig. 2C). After cloning the DNA fragment into the pCR2.1-TOPO vector, the nucleotide sequence of exon II was determined. Figure 2D shows the sequence of the complementary strand of exon II of the affected fibrinogen Bβ chain gene in which C was identified instead of A at position 3356. Four out of seven clones had C whereas three clones had A at this position. These data indicated that there was a heterozygous T→G mutation at position 3356 of the patient fibrinogen Bβ chain gene.

This nucleotide mutation should introduce an NheI recognition sequence (GCTAGC) at this position. Therefore, susceptibility of PCR-amplified exon II DNA fragments to NheI was investigated by incubation with NheI followed by agarose gel electrophoresis analysis. As shown in Fig. 3, the PCR-amplified 392-bp DNA fragment of exon II derived from the patient fibrinogen Bβ chain gene was partially cleaved by NheI resulting in 248- and 144-bp fragments. In contrast, the corresponding fragment amplified from a normal fibrinogen Bβ chain gene was not cleaved by NheI. Similarly, the PCR-amplified 4.9-kbp

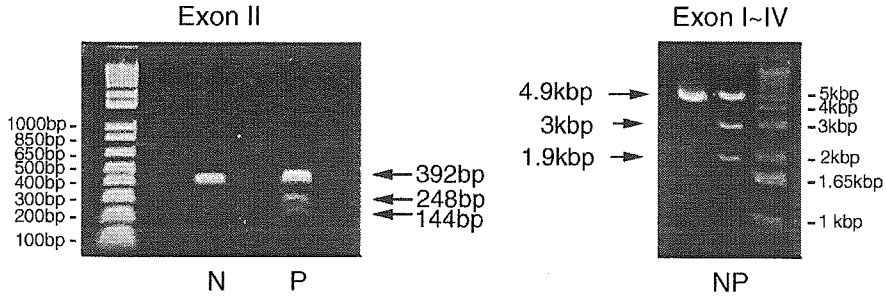

Fig. 3. Restriction fragment length polymorphism of polymerase chain reaction (PCR)-amplified DNA fragments. The PCR-amplified DNA fragments (N, normal; P, patient) of exon II and those of exons I, II, III, and IV including introns were incubated in the presence of NheI (10 U) and then analyzed by agarose gel electrophoresis. Arrows indicate PCR-amplified DNA fragments and the NheI cleaved DNA fragments. Lengths of these DNA fragments and molecular markers (1-kb DNA Ladder, Invitrogen) are shown on the side of DNA fragments.

DNA fragment, including exons I, II, III, and IV and introns, derived from the patient fibrinogen Bβ chain gene was partially cleaved by NheI resulting in 3.0-kbp and 1.9-kbp fragments, whereas that derived from a normal fibrinogen Bβ chain gene was not digested by NheI. The observation that two DNA fragments amplified by PCR using two independent primer pairs were susceptive to NheI confirmed that the heterozygous NheI recognition sequence in exon II of patient fibrinogen Bβ chain gene was not an artefact of PCR. The T→G mutation at position 3356 of the patient fibrinogen Bβ chain gene caused a nonsense mutation (TAT sequence for Bβ Tyr41 to TAG sequence for translation termination signal) resulting in truncation of the affected fibrinogen Bβ chain.

Discussion

Molecular mechanisms of congenital hypofibrinogenemia may be assigned to a variety of genetic mutations such as deletion of nucleotides, insertion of nucleotides, nonsense mutations, or missense mutations in one of the fibrinogen genes. Four Aα chain gene mutations causing truncations of the affected Aα chains [6] and a nonsense mutation, which result in early truncation of the γ chain, have been reported [7]. Patients with missense mutations develop not only dysfibrinogenemia, but also hypofibrinogenemia [4,8–11]. For example, the γ284 Gly→Arg mutation causes an intracellular transport defect of the molecule resulting in accumulation of the affected fibrinogen molecules in the endoplasmic reticulum [11]. In addition, the γ82 Ala→Gly and Bβ316 Asp→Tyr mutations result in hypofibrinogenemia without expression of variant molecules in plasma [9,11]. Here we report a new nonsense mutation in the patient fibrinogen Bβ chain gene that results in an early truncation of the fibrinogen Bβ chain. The C-terminal end of the affected fibrinogen Bβ chain molecule is predicted to be Bβ Gly-40. Incorporation of such a shorter chain into the fibrinogen molecule depends on the truncation site. Since the truncated polypeptide derived from the affected Bβ chain gene has no Cys residues, it will not be assembled with other fibrinogen chain molecules by disulfide bridges. In this heterozygous patient, the plasma fibrinogen level was 99.2 mg dL^{-1} and no abnormal fibrinogen molecules were detected in patient plasma, so that coagulation reactions should not be greatly perturbed. However, this genetic mutation may result in afibrinogenemia in a homozygous patient.

References

1 Henshen A, Lottspeich F, Kehl M, Southern C. Covalent structure of fibrinogen. *Ann NY Acad Sci* 1983; **408**: 28–43.

2 Doolittle RF. Fibrinogen and fibrin. *Ann Rev Biochem* 1984; **53**: 195–299.

3 Huang S, Mulvihill ER, Farrell DH, Davie EW. Biosynthesis of human fibrinogen: subunit interactions and potential intermediates in the assembly. *J Biol Chem* 1993; **268**: 8919–26.

4 Brennan SO, Fellowes AP, George PM. Molecular mechanisms of hypo- and afibrinogenemia. *Ann NY Acad Sci* 2001; **936**: 91–100.

5 Mimuro J, Kawata Y, Niwa K, Muramatsu S, Madoiwa S, Takano H, Sugo T, Sakata Y, Sugimoto T, Nose K, Matsuda M. A new type of ser substitution or γArg-275 in fibrinogen Kamogawa I characterized by impaired fibrin assembly. *Thromb Haemost* 1999; **81**: 940–4.

6 Fellowes AP, Brennan SO, Holme R, Stormorken H, Brosstad FR, George PM. Homozygous truncation of the fibrinogen Aα chain within the coiled coil causes congenital afibrinogenemia. *Blood* 2000; **96**: 773–5.

7 Okumura N, Terasawa F, Yonekawa O, Hamada E, Kaneko H. Hypofibrinogenemia associated with a heterozygous C→T nucleotide substitution at position −1138 BP of the 5′-flanking region of the fibrinogen A α-chain gene. *Ann NY Acad Sci* 2001; **936**: 526–30.

8 Terasawa F, Okumura N, Kitano K, Hayashida N, Shimosaka M, Okazaki M, Lord ST. Hypofibrinogenemia associated with a heterozygous missense mutation 153Cys to Arg (Matsumoto IV): *in vitro* expression demonstrates defective secretion of the variant fibrinogen. *Blood* 1999; **94**: 4122–31.

9 Brennan SO, Fellowes AP, Faed JM, George PM. Hypofibrinogenemia in an individual with 2 coding (γ82 A→G and Bβ235 P→L) and 2 noncoding mutations. *Blood* 2000; **95**: 1709–13.

10 Brennan SO, Wyatt J, Medicina D, Callea F, George PM. Fibrinogen Brescia: hepatic endoplasmic reticulum storage and hypofibrinogenemia because of a γ284 Gly→Arg mutation. *Am J Pathol* 2000; **157**: 189–96.

11 Brennan SO, Wyatt JM, May S, De Caigney S, George PM. Hypofibrinogenemia due to novel 316 Asp→Tyr substitution in the fibrinogen Bβ chain. *Thromb Haemost* 2001; **85**: 450–3.

In Vitro Platelet Activation by an Echo Contrast Agent

Kouichirou Shigeta, MD, Nobuyuki Taniguchi, MD, PhD, Kiyoka Omoto, MD, PhD, Seiji Madoiwa, MD, PhD, Yoichi Sakata, MD, PhD, Masaki Mori, MD, PhD, Kiyohiko Hatake, MD, PhD, Kouichi Itoh, MD, PhD

Objective. We investigated whether an ultrasonic echo contrast agent containing microbubbles (Levovist [SH U 508A]; Schering AG, Berlin, Germany) could in routine use activate platelets. ***Methods.*** Levovist and its main component, galactose, were mixed with separate samples of whole blood (1.5–75 mg/mL) from 5 healthy volunteers to form a 1-mL suspension sample. After in vitro exposure to ultrasound emitted from a commercial ultrasonic scanner at a pulse frequency of 3.5 MHz with a mechanical index of 1.9 and an exposure duration of 5 minutes, 5 μL of the sample was incubated for 20 minutes with the fluorescein isothiocyanate-labeled CD61 antibody, which is a platelet-specific antigen, and the phycoerythrin-labeled CD62P (P-selectin) antibody, an activation-specific antigen, both on the platelet surface. After more than 30 minutes of fixing in 1% paraformaldehyde, flow cytometric analysis was performed. ***Results.*** The percentage of CD62P-expressing platelets increased according to the concentrations of Levovist and galactose, which showed almost equal effects. Ultrasound exposure did not enhance the effect except at the highest concentration of Levovist (75 mg/mL). ***Conclusions.*** In vitro, a galactose-based echo contrast agent could not activate the platelets at its routine concentration. ***Key words:*** CD62P; echo contrast agents; in vitro; platelet activation; ultrasound.

Abbreviations
ADP, adenosine diphosphate; FITC, fluorescein isothiocyanate; GLUT, glucose transporter; MCV, mean cellular volume; MI, mechanical index; MPV, mean platelet volume; PE, phycoerythrin; RBC, red blood cell

Received April 2, 2002, from the Departments of Clinical Laboratory Medicine (K.S., N.T., K.O., K.I.) and Hematology (M.M., K.H.) and Division of Cell and Molecular Medicine, Center for Molecular Medicine (S.M., Y.S.), Jichi Medical School, Tochigi-ken, Japan. Revision requested May 8, 2002. Revised manuscript accepted for publication December 5, 2002.

Address correspondence and reprint requests to Kouichirou Shigeta, MD, Department of Clinical Laboratory Medicine, Jichi Medical School, 3311-1 Yakusiji, Minamikawachi-machi, Kawachi-gun, Tochigi-ken 329-0498, Japan.

Echo contrast agents, which consist of microbubbles of galactose, albumin, and other substances, have been developed to improve the sonographic imaging of tissues, and their action as cavitation nuclei has also been studied.[1–4] Pulsed ultrasound in the 1- to 10-MHz frequency range can, through resonance, expand and collapse microbubbles violently enough to damage formed elements of the blood and the tissues of the internal organs, a process known as transient acoustic cavitation or inertial cavitation.[5] Cavitation-related bioeffects can include hemolysis,[6] blood vessel damage in organs,[7,8] and DNA damage in cultured cells.[9]

The platelets play important roles not only in hemostasis but also when activated in the formation of atherosclerotic lesions in blood vessels. Platelets circulate in their resting state, in which they are spherical and are activated by coagulation factors such as thrombin, thromboxane A2, and adenosine diphosphate (ADP) or by mechanical forces such as shear stress.[10] Activated platelets extend pseudopodia and release their granules, which contain cytokines and coagulation factors. They

contribute to blood coagulation and to the migration and proliferation of smooth muscle cells and monocytes.[11]

There are many reports of the action of ultrasound on platelets. High-intensity focused ultrasound causes activation, aggregation, and adhesion of platelets.[12] Platelets were induced by ultrasound to form aggregates around gas-filled pores in membranes immersed in platelet-rich plasma.[13] The platelet-specific protein β-thromboglobulin was released by ultrasound at therapeutic intensities.[14] Furthermore, the action of ultrasound on the microbubbles in echo contrast agents can cause platelet lysis.[15] Previous study conditions for cavitation were rather specialized: low counts of formed elements (e.g., blood with 5% hematocrit or platelet-rich plasma alone), longer pulse durations, and lower frequencies than used clinically. The bioeffects of platelet activation have not been studied under routine sonographic diagnostic conditions. The purpose of our study was to determine whether the inclusion of microbubbles in echo contrast agents could affect the activation of platelets. We examined their interaction in diagnostic use in vitro.

Materials and Methods

Basic Study

Blood Collection and In Vitro Agonist Stimulation of Platelets

Three healthy men, 30, 34, and 38 years of age, who were nonsmokers and had not taken any antithrombotic drugs for at least 10 days, were examined after informed consent was obtained. Freshly donated blood was treated with 1 mL of 0.13-mol sodium citrate (pH 5.0) per 10 mL of blood to prevent coagulation. The citrated whole blood was incubated with ADP (A-9665; Sigma-Aldrich Corp, St Louis, MO) at concentrations of 0.1 to 1000 μmol/L for 5 minutes at room temperature without agitation to confirm platelet reactivity and analyzed using a flow cytometer.

Cell Counts After Mixing With Contrast Agent or Galactose

The contrast agent Levovist (SH U 508A; Schering AG, Berlin, Germany) at a quantity of 2.5 g was dissolved in 7 mL of distilled water so that the final concentration was 300 mg/mL, and the solution was used within 15 minutes. In addition, 2.5 g of D(+)-galactose (Kanto Chemical Co, Inc, Tokyo, Japan) was mixed with 7 mL of distilled water to give a final concentration of 300 mg/mL. The fresh Levovist and galactose solutions were carefully mixed with citrated whole blood to yield concentrations of 1.5, 15, and 75 mg/mL. The number of blood cells per microliter (referred to below as blood cell counts) of each sample, the mean cellular volume (MCV) of red blood cells (RBCs), and the mean platelet volume (MPV) were determined in each sample with a hematologic analyzing system (STKS-Retic; Beckman Coulter, Inc, Fullerton, CA) before and after being mixed with Levovist or galactose for 5, 15, and 30 minutes.

Changing Duration After Ultrasound Exposure and Mechanical Index

Samples (1 mL) of Levovist at a concentration of 75 mg/mL were placed in 2-mL polyester centrifuge tubes (8 mm in internal diameter, 0.25 mm in wall thickness; Beckman Coulter, Inc), which were reported to be sufficiently acoustically transparent at frequencies of 1 to 5 MHz.[14] The loaded tubes were placed 5 cm from the transducer in a container filled with degassed water at room temperature and moved manually up and down through the imaging plane to help ensure exposure of the cell suspension. The container was made of an acryl board 4 mm in thickness and measured 15 × 15 × 10 cm.

The ultrasonic pulses with a center frequency of 3.5 MHz were focused on the sample from the diagnostic scanner (Acuson Sequoia 512; Siemens Medical Solutions, Mountain View, CA) with a model 5V2c sector-type transducer (whose focus was set at a depth of 5 cm). The exposure conditions were B-mode, a mechanical index (MI) of 1.9, a pulse duration of 0.84 μsec (which covers 3 cycles), and a pulse repetition cycle of 2870 Hz. We recognize that the use of the MI was limited as an exposure parameter but was necessary, because measurements of acoustic output from the systems were otherwise unavailable to us. The samples containing Levovist at a concentration of 75 mg/mL were exposed to ultrasound for 5 minutes, and the CD62P (P-selectin) expression rates were determined immediately and after 5 and 10 minutes with a flow cytometer to ascertain time dependency.

The samples with Levovist at 75 mg/mL were exposed to ultrasound (MI, 0 [sham], 0.5, 1.0, 1.5, and 1.9) for 5 minutes, and CD62P expression was determined with the flow cytometer to study the dependency on the ultrasonic power.

Main Study Procedure

Blood Collection and Levovist, Galactose, Ultrasound, and ADP Exposure

Five healthy men (23–38 years old; mean, 30.4 years), 3 of whom also participated in the basic study, were examined under the same conditions as in the basic study after giving their informed consent. Blood was collected as citrated whole blood, and fresh Levovist solution was mixed in carefully to make up samples of 1 mL. Final concentrations of 1.5, 15, 30, 45, and 75 mg/mL were obtained by adding 5, 50, 100, 150, and 250 μL of fresh Levovist solution to 995, 950, 900, 850, and 750 μL of citrated whole blood, respectively. Each sample was sham exposed or exposed (MI, 1.9) to the scanner for 5 minutes, and then each sample was incubated with or without ADP at 10 μmol/L for 5 minutes, and the CD62P expression was analyzed by flow cytometry (Fig. 1). Galactose was mixed with citrated whole blood at concentrations of 1.5, 15, 30, 45, and 75 mg/mL without addition of ADP or exposed to ultrasound, and the CD62P expression was analyzed by flow cytometry.

Figure 1. Experiments in the main study. Citrated whole blood was mixed with Levovist and galactose at concentrations of 0, 1.5, 15, 30, 45, and 75 mg/mL, exposed to ultrasound (US), and incubated with ADP. The blood cells in each sample were counted and analyzed on a flow cytometer.

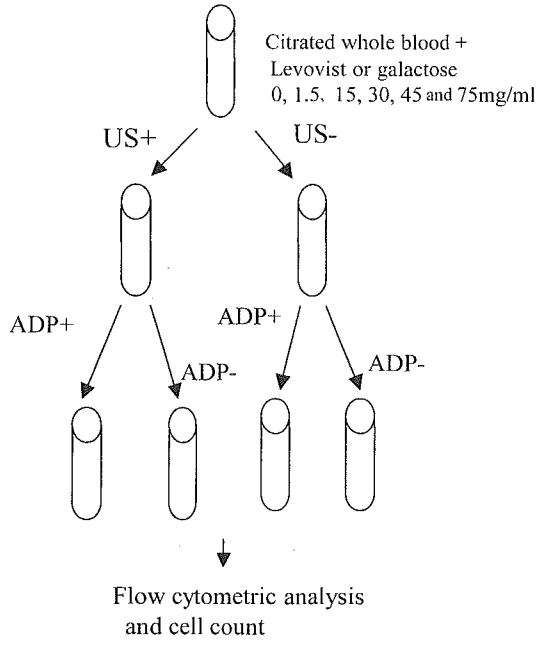

Antibodies

CD61 is a marker of platelet glycoprotein IIIa, which is found on both normal (resting) and activated platelets. We used murine antihuman monoclonal fluorescein isothiocyanate (FITC)-conjugated CD61 (Becton, Dickinson and Company, San Jose, CA) to identify all platelets. CD62P is found on the external membrane of activated platelets after α granule secretion. Murine antihuman monoclonal phycoerythrin (PE)-conjugated CD62P (Becton, Dickinson and Company) was used to detect platelet activation. Isotype controls were run in parallel with all monoclonal antibodies: FITC-conjugated immunoglobulin G1 (BD34041; Becton, Dickinson and Company) and PE-conjugated immunoglobulin G1 (BD34013; Becton, Dickinson and Company).

Preparation of Samples for Flow Cytometry

Each sample of 5 μL was transferred to a tube containing a mixture of 10 μL of FITC-conjugated CD61 antibody and 10 μL of PE-conjugated CD62 antibody and was incubated for 20 minutes in the dark at room temperature. Then 1 mL of ice-cold 1% paraformaldehyde was added to the tube, which was placed in the dark at 4°C for more than 30 minutes, and the samples were analyzed on a flow cytometer. For the flow cytometric analysis, samples must be placed in the dark in an ice-cold situation.

Flow Cytometric Analysis

Flow cytometric analysis was performed on a FACScan (Becton, Dickinson and Company) equipped with an argon ion laser and CellQuest software (Becton, Dickinson and Company). Cytometer performance was verified with FITC and PE calibration beads (Becton, Dickinson and Company; and Flow Cytometry Standards Corporation, Research Triangle Park, NC). Forward light scatter and 2 fluorescent signals were determined for each cell, and 4000 platelet events were inserted into the list mode data files. The platelet population was logic gated by a forward scatter versus side scatter dot plot gate and by an FITC-conjugated CD61 versus side scatter dot plot gate. CD62P-positive activated platelets were identified by fluorescein intensity greater than that of the appropriate isotype control staining sample. The frequencies of CD62P-positive platelets were expressed as percentages of the total platelet population.

Statistical Analysis

Data are represented as mean ± SD unless otherwise stated. Statistical differences were determined by the paired Student t test. $P < .05$ was considered significant.

Results

Basic Study

When the platelets were activated with ADP, the platelet activation rate assessed from CD62P expression increased as the concentration of ADP increased, reaching about 60% at a maximal ADP concentration of 1000 µmol/L. We used ADP at 10 µmol/L in the main study (discussed below) because the expression rate was intermediate, which was appropriate for this study (Fig. 2).

After the Levovist sample (75 mg/mL) was exposed to ultrasound (MI, 1.9) for 5 minutes, there was no difference in the CD62P expression rate immediately (0 minutes) and after 5 and 10 minutes. We measured the CD62P expression immediately after exposure to ultrasound in the main study using Levovist (Fig. 3).

The expression rate increased with the power of the ultrasound (MI) but had almost the same values at MIs of 1.5 and 1.9 (Fig. 4).

Blood cell counts after mixing with Levovist concentrations of 1.5, 15, and 75 mg/mL are presented in Table 1. Red blood cell counts did not change significantly in these procedures; however, the platelet counts decreased slightly at 30 minutes in Levovist at a concentration 15 mg/mL and significantly at 5, 15, and 30 minutes at 75 mg/mL. The MCV decreased at 30 minutes in Levovist at 1.5 mg/mL and increased significantly at 5, 15, and 30 minutes at 75 mg/mL. The MPV increased significantly at 30 minutes in Levovist at 1.5 mg/mL, at 15 and 30 minutes at 15 mg/mL, and at 5, 15, and 30 minutes at 75 mg/mL. The effects of galactose on RBC and platelets were almost the same as those at the same concentration of Levovist (75 mg/mL; Table 1).

Main Study

CD62P expression increased with the concentration of the Levovist (Fig. 5). The maximal percentage of CD62P expression, 55%, was seen at a Levovist concentration of 75 mg/mL and was significantly greater than that in the control. At concentrations between 1.5 and 45 mg/mL, there was no significant difference from the control. When the expression rate after ultrasound exposure was compared with that without exposure, CD62P expression was significantly increased in the exposed group only at the highest concentration (75 mg/mL). The highest concentration was approximately 5 times clinical levels.

In the study in which the ADP solution at a concentration of 10 µm/L was added, the CD62P expression rate increased at all concentrations both with and without ultrasound exposure. A significant synergistic effect compared with the control (Fig. 6) was observed at concentrations of Levovist from 30 to 75 mg/mL, but no significant difference was observed at concentrations of 1.5 and 15 mg/mL. When results with ultrasound exposure were compared with those with no exposure, no significant difference in CD62P expression was observed at any concentration.

Figure 2. Effect of ADP on CD62P expression on platelets in vitro. Citrated whole blood was mixed with the ADP solutions at concentrations of 0.1, 1, 10, 100, 500, and 1000 µmol/L for 5 minutes. Bars represent actual percentages of CD62P-expressing platelets.

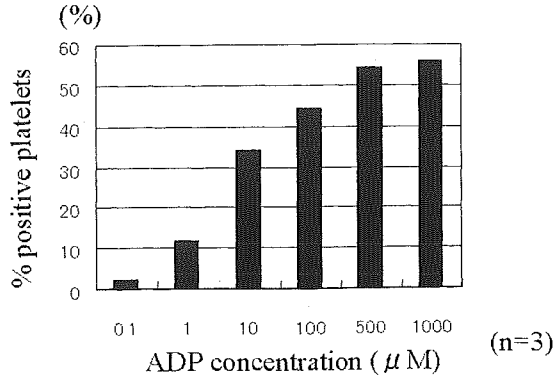

Figure 3. CD62P expression on platelets after ultrasound exposure. Citrated whole blood was mixed with Levovist at 75 mg/mL and exposed to ultrasound for 5 minutes, and CD62P was measured immediately (0) and after 5 and 10 minutes. Bars represent actual percentages of CD62P-expressing platelets.

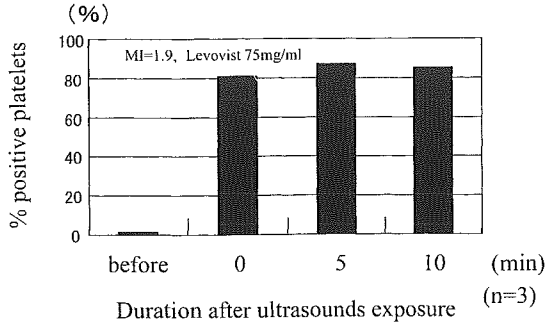

The CD62P expression rate also increased according to the concentration of galactose, but it was almost the same as that in the Levovist experiment. The difference was greater at the highest concentrations of Levovist and galactose (Fig. 7)

A representative pair of contour plots of platelets is presented in Figure 8. The dots in the top right quadrant of each contour plot represent CD61-positive platelets that coexpress the activation marker CD62P. The results from the Levovist sample at 75 mg/mL exposed to ultrasound are on the right, showing an expression rate of 88.2%, and those of the Levovist sample at 75 mg/mL without exposure are on the left, with an expression rate of 80.2%.

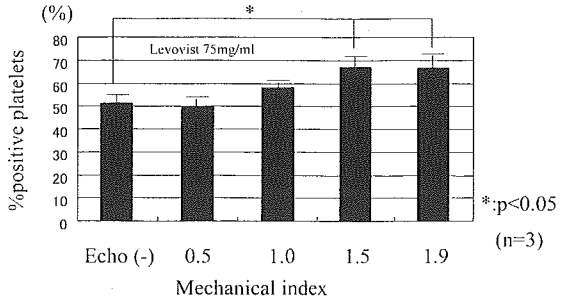

Figure 4. CD62P expression on platelets after changes in MI. Citrated whole blood was mixed with Levovist at 75 mg/mL and exposed to ultrasound for 5 minutes, and the MI was varied between 0 and 1.9. 0 indicates no exposure to ultrasound. Bars represent actual percentages of CD62P-expressing platelets.

Discussion

Our study showed that galactose-based echo contrast agents could not activate platelets at their clinical concentrations. If microbubbles collapse violently, mechanical effects may arise through an erosion process, through the growth of intracellular bubbles, or through acoustic microstreams; also, a rising temperature could affect the cells.[16] Platelets have a diameter of less than half that of RBCs, so they can be expected to be more resistant to the shear forces that accompany violent bubble collapse.[17] Moreover, damage to the platelet membrane does not result in platelet lysis but may affect platelet function.[18,19]

Recently, several monoclonal antibodies that recognize platelet surface antigens have been developed.[20–23] Activated platelets express activation-specific antigens on the platelet surface, for example, PAC-1, and CD62P. PAC-1 is used for the detection of activation of glycoprotein IIb-IIIa, which binds to fibrinogen, and CD62P is used for detection of α granule degranulation. CD62P has

Table 1. Blood Cell Counts and Volumes After Mixing Blood With Levovist and Galactose

Agent	Count	Before	After 5 min	After 15 min	After 30 min
Levovist					
1.5 mg/mL	RBC*	4.42 ± 2.01	4.42 ± 1.02	4.36 ± 0.577	4.41 ± 0.33
	MCV, fL	90.3 ± 0.56	90.0 ± 3.3	89.3 ± 0.56	89.3 ± 0.56
	Plt†	17.6 ± 0.10	17.3 ± 0.06	17.2 ± 0.06	17.0 ± 0.52
	MPV, fL	6.93 ± 0.06	6.98 ± 0.12	7.11 ± 0.06	7.34 ± 0.06‡
15 mg/mL	RBC*	4.33 ± 0.57	4.33 ± 0.52	4.33 ± 0.1	4.34 ± 0.57
	MCV, fL	89.6 ± 0.56	90.6 ± 0.57	91.0 ± 0.33‡	91.3 ± 0.56‡
	Plt†	18.9 ± 0.06	17.8 ± 0.25	15.9 ± 0.66	15.7 ± 0.52‡
	MPV, fL	6.93 ± 0.12	7.87 ± 0.05	8.13 ± 0.05‡	8.17 ± 0.25‡
75 mg/mL	RBC*	3.44 ± 1.12	3.45 ± 0.58	3.46 ± 0.56	3.45 ± 0.57‡
	MCV, fL	89.3 ± 0.56	108.6 ± 0.57‡	123.0 ± 0.57‡	146.7 ± 0.56‡
	Plt†	14.8 ± 0.10	9.9 ± 0.06‡	9.8 ± 0.06‡	8.7 ± 0.12‡
	MPV, fL	6.83 ± 0.06	8.3 ± 0.10‡	8.23 ± 0.12‡	8.77 ± 0.06‡
Galactose					
75 mg/mL	RBC*	3.35 ± 1.1	3.28 ± 1.53	3.33 ± 0.36	3.34 ± 1.57‡
	MCV, fL	89.3 ± 2.56	107.7 ± 2.57‡	120.0 ± 1.07‡	145.7 ± 1.52‡
	Plt†	12.8 ± 0.10	10.2 ± 0.06‡	9.8 ± 0.31‡	8.8 ± 0.10‡
	MPV, fL	7.4 ± 0.16	8.2 ± 0.10‡	8.33 ± 1.52‡	8.87 ± 0.06‡

Citrated whole blood was mixed with Levovist and galactose at concentrations of 1.5, 15, and 75 mg/mL, and the blood cells were counted at 3 time points (5, 15, and 30 min). For galactose, only the results for the 75 mg/mL concentration are shown. Data are mean ± SD.

*Values are $\times 10^6/mm^3$.

†Plt indicates platelets. Values are $\times 10^4/mm^3$.

‡Differences were significant compared with before the treatment ($P < .05$).

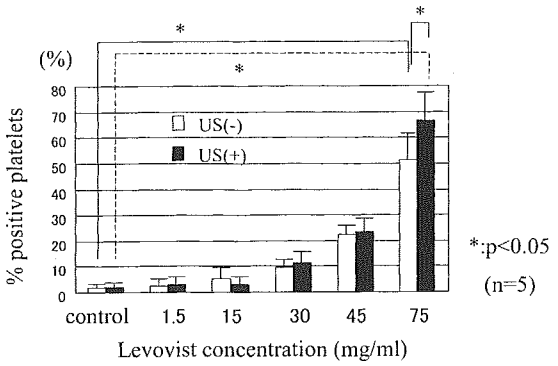

Figure 5. Effect of Levovist concentration and ultrasound exposure on CD62P expression on platelets. Citrated whole blood was mixed with Levovist at concentrations of 1.5, 15, 30, 45, and 75 mg/mL. Open and filled bars represent the nonuse and use of ultrasound, respectively, and show actual percentages of CD62P expression. Asterisks indicate significant differences ($P < .05$).

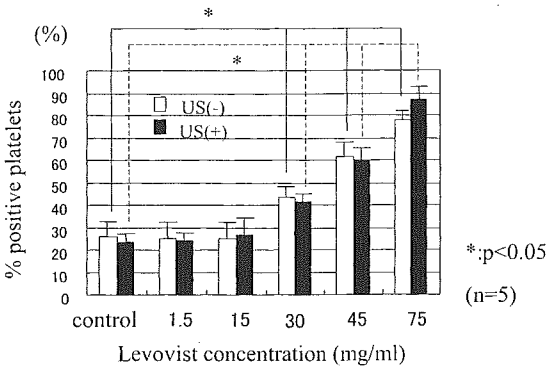

Figure 6. Synergistic effect of ADP on Levovist-induced CD62P expression on platelets. Citrated whole blood was mixed with ADP solution at 10 μmol/L plus Levovist at 1.5, 15, 30, 45, and 75 mg/mL. Open and filled bars represent the nonuse and use of ultrasound, respectively, and show actual percentages of CD62P expression. Asterisks indicate significant differences compared with control.

higher thresholds for ADP than does PAC-1[24] and changes the expression rate in a dose-dependent manner, so it was better as a marker for platelet activation in this study. Antibodies for these specific antigens on the platelet surface can be used for detecting activated platelets by flow cytometry.[25] Flow cytometry is likely to be considerably more useful for studies of platelet reactivity than assays of biochemical markers of activation, including platelet factor 4 and β-thromboglobulin.[26] Using this method, several investigators have found platelet activation in patients who underwent cardiopulmonary bypass surgery or who had coronary artery disease and other diseases.[27–29] Therefore, we used the anti-CD62P antibody to detect activated platelets by flow cytometry.

Figure 7. Effect of concentrations of Levovist and galactose on CD62P expression on platelets. Citrated whole blood was mixed with Levovist (filled squares) and galactose (open squares) at 1.5, 15, 30, 45, and 75 mg/mL. Each square represents the actual percentage of CD62P expression.

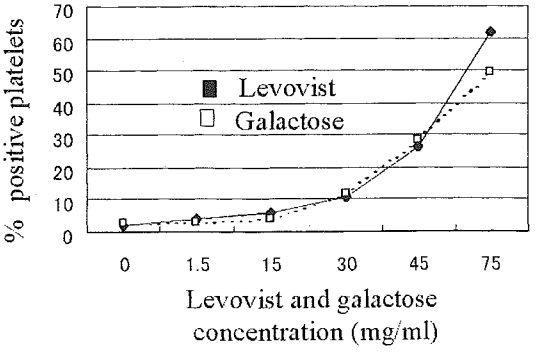

In this study we investigated whether a microbubble echo contrast agent exposed to ultrasound could activate platelets in a routine clinical situation. Although a dose-dependent increase in CD62P expression in response to Levovist and galactose was shown between concentrations of 1.5 and 15 mg/mL, which are thought to be practical for clinical use,[6] CD62P expression increased slightly but not significantly. Levovist and galactose showed the potential to activate platelets at the high concentration (75 mg/mL, approximately 5 times clinical levels). Ultrasound showed no enhancement effects except at the high concentration (75 mg/mL).

The presence of ADP enhanced the effect, suggesting that the destruction of platelets in vivo could lead to enhanced platelets. Adenosine diphosphate is contained in the dense body of the platelet, is excreted after platelet activation, and can itself activate platelets. CD62P expression increased significantly compared with the control at Levovist concentrations higher than 30 mg/mL but did not increase at concentrations for practical use.

At the maximal concentration of Levovist, CD62P expression increased with the MI but reached a plateau at MIs of greater than 1.5. This may indicate that the platelet activation mechanism of ultrasound has a threshold resulting from a cavitationlike effect.[30]

In the blood cell counts after the addition and mixing of Levovist or galactose, the RBC count showed no change, but the platelet count decreased with increasing concentrations of

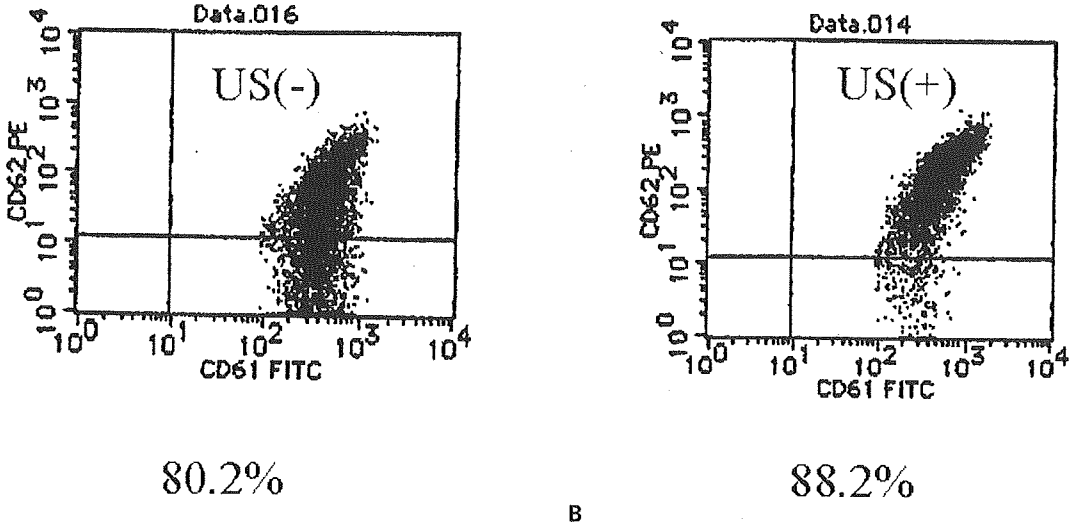

Figure 8. Flow cytometric dot plot of platelets without (**A**) and with (**B**) ultrasound exposure in samples containing Levovist. Citrated whole blood was mixed with Levovist at 75 mg/mL and exposed to ultrasound (MI, 1.9). The platelet population is expressed as a dot plot resulting from the gating of FITC-conjugated CD61 versus PE-conjugated CD62P. The number under each contour plot represents the percentage of CD61-positive platelets that coexpress the activation marker CD62P.

either of the 2 solutes. Both the MCV of RBCs and the MPV increased with Levovist and galactose concentrations. Levovist consists of 99.9% galactose and 0.1% palmitic acid, and the results were almost the same for both Levovist and galactose. Red blood cells and platelets express the glucose transporter (GLUT) isoforms GLUT1[31] and GLUT3,[32] respectively. GLUT1 and GLUT3 are known to transport not only glucose but also galactose into RBCs and platelets. Transported galactose is changed predominately into galactitol by aldose reductase because galactose is a better substrate for aldose reductase than glucose, and the stored galactitol in the cells can cause cellular damage via processes such as osmotic dysregulation,[33,34] which may be one reason for the activation of platelets.

Although Levovist could activate platelets at the high concentration, to our knowledge, no hemostatic complication in the use of Levovist has been reported. Considering that the maximal clinical concentration is about 15 mg/mL,[6] it may not be possible to activate platelets under normal conditions. Moreover, ultrasound is attenuated in the human body, and that effect occurs far less in vitro, so it is probably not powerful enough to cause damage in vivo. We performed this study in vitro, but now an in vivo study of the possibility of the platelet activation is necessary to ensure the safety of contrast-enhanced sonography.

References

1. Church CC. The effects of an elastic solid surface layer on the radial pulsations of gas bubbles. J Acoust Soc Am 1995; 97:1510–1521.
2. de Jong N, Hoff L. Ultrasound scattering properties of Albunex microspheres. Ultrasonics 1993;31:175–181.
3. Holland CK, Apfel RE. Thresholds of transient cavitation produced by pulsed ultrasound in a controlled nuclei environment. J Acoust Soc Am 1990; 88: 2059–2069.
4. Lotsberg O, Hovem JM, Aksum B. Experimental observation of subharmonic oscillations in Infoson bubbles. J Acoust Soc Am 1996; 99:1366–1369.
5. Crum LA, Roy RA, Dinno MA, et al. Acoustic cavitation produced by microsecond pulses of ultrasound: a discussion of some selected results. J Acoust Soc Am 1992; 91:1113–1119.
6. Williams AR, Kubowicz G, Cramer E, Schlief R. The effects of the microbubble suspension SH U 454 (Echovist) on ultrasound-induced cell lysis in a rotating tube exposure system. Echocardiography 1991; 8:423–433.
7. Carstensen EL, Kelly P. Church CC, et al. Lysis of erythrocytes by exposure to CW ultrasound. Ultrasound Med Biol 1993; 19:147–165.

8. Penney DP, Schenk EA, Maltby K, et al. Morphological effects of pulsed ultrasound in the lung. Ultrasound Med Biol 1993; 19:127–135.

9. Kondo T, Kodaira T, Kano E. Free radical formation induced by ultrasound and its effects on strand breakage in DNA of cultured FM3A cells. Free Radic Res Commun 1993; 19:S193–S200.

10. Ikeda Y, Handa M, Kawano K, et al. The role of von Willebrand factor and fibrinogen in platelet aggregation under varying shear stress. J Clin Invest 1991; 87:1234–1240.

11. Ross R. Atherosclerosis: an inflammatory disease. N Engl J Med 1999; 340:115–126

12. Pollachik SL, Chandler WL, Mourad PD, Ollos RL, Crum LA. Activation, aggregation and adhesion of platelets exposed to high-intensity focused ultrasound. Ultrasound Med Biol 2001; 27:1567–1576.

13. Miller DL, Nyborg WL. Platelet aggregation induced by ultrasound under specialized conditions in vitro. Science 1979; 205:505–507.

14. Williams AR, Chater BV, Allen KA, Sherwood MR, Sanderson JH. Release of β-thromboglobulin from human platelets by therapeutic intensities of ultrasound. Br J Haematol 1978; 40:133–142.

15. Everbach EC, Makin IR, Francis CW, Meltzer RS. Effect of acoustic cavitation on platelets in the presence of an echo-contrast agent. Ultrasound Med Biol 1998; 24:129–136.

16. Leighton TG. The Acoustic Bubble. London, England: Academic Press; 1994.

17. Skalak R, Chien S. Handbook of Bioengineering. New York, NY: McGraw-Hill; 1987.

18. Charter BV, Williams AR. Platelet aggregation induced in vitro by therapeutic ultrasound. Thromb Haemost 1977; 38:640–651.

19. Williams AR, O'Brien WD, Coller JR. Exposure to ultrasound decreases the recalcification time of platelet rich plasma. Ultrasound Med Biol 1976; 2: 113–118.

20. Berman CL, Yeo EL, Wencel-Drake JD, et al. A platelet alpha granule membrane protein that is associated with the plasma membrane after activation: characterization and subcellular localization of platelet activation-dependent granule-external membrane protein. J Clin Invest 1986; 78:130–137.

21. Nieuwenhuis HK, van Oosterhout JJG, Rozemuller E, van Iwaarden F, Sixma JJ. Studies with a monoclonal antibody against activated platelets: evidence that a secreted 53,000-molecular weight lysosomal-like granule protein is exposed on the surface of activated platelets in the circulation. Blood 1987; 70:838–845.

22. McEver RP, Martin MN. A monoclonal antibody to a membrane glycoprotein binds only to activated platelets. J Biol Chem 1984; 259:9799–9804.

23. Metzelaar MJ, Wijngaard PLJ, Peters PJ, Sixma JJ, Nieuwenhuis HK, Clevers HC. CD63 antigen: a novel lysosomal membrane glycoprotein, cloned by a screening procedure for intracellular antigens in eukaryotic cells. J Biol Chem 1991; 266:3239–3245.

24. Holmes MB, Sobel BE, Howard DB, Schneider DJ. Difference between activation thresholds for platelet P-selectin and glycoprotein IIb-IIIa expression and their clinical implications. Thromb Res 1999; 95:75–82.

25. Shattil SJ, Cunningham M, Hoxie JA. Detection of activated platelets in whole blood using activation dependent monoclonal antibodies and flow cytometry. Blood 1987; 70:307–315.

26. Schneider D, Tracy PB, Mann KG, Sobel BE. Differential effects of anticoagulations on the activation of platelets ex vivo. Circulation 1997; 96:2877–2883.

27. George JN, Pickett EB, Saucerman S, et al. Platelet surface glycoproteins: studies on resting and activated platelets and platelet membrane microparticles in normal subjects, and observation in patients during adult respiratory distress syndrome and cardiac surgery. J Clin Invest 1986; 78:340–348.

28. Knight CJ, Panesar M, Wright C, et al. Altered platelet function detected by flow cytometry: effect of coronary artery disease and age. Arterioscler Thromb Vasc Biol 1997; 17:2044–2053.

29. Rinder CS, Bohnert J, Rinder HM, Michell J, Ault K, Hillman R. Platelet activation and aggregation during cardiopulmonary bypass. Anesthesiology 1991; 75:388–393.

30. Miller DL, Williams AR. Bubble cycling as the explanation of the promotion of ultrasonic cavitation in a rotating tube exposure system. Ultrasound Med Biol 1989; 15:641–648.

31. Longo N, Elsas L. Human glucose transporters. Adv Pediatr 1998; 45:293–313.

32. James DC, Michael S, Christopher IC. GLUT-3 (brain-type) glucose transporter polypeptides in human blood platelets. Thromb Res 1995; 15:461–469.

33. Engerman RL, Kern TS. Experimental galactosemia produces diabetic-like retinopathy. Diabetes 1984; 33:97–100.

34. Takahashi Y, Wyman M, Ferris F III, Kador PF. Diabetes-like preproliferative retinal changes in galactose-fed dogs. Arch Ophthalmol 1992; 110:1295–1302.

Defective Sorting to Secretory Vesicles in Trans-Golgi Network Is Partly Responsible for Protein C Deficiency

Molecular Mechanisms of Impaired Secretion of Abnormal Protein C R169W, R352W, and G376D

Masao Naito, Jun Mimuro, Hitoshi Endo, Seiji Madoiwa, Kyo-ichi Ogata, Jiro Kikuchi, Teruko Sugo, Takanori Yasu, Yusei Kariya, Yuichi Hoshino, Yoichi Sakata

Abstract—Three thrombophilic patients with protein C (PC) deficiency were found to have independent mutations in the PC gene. These mutations resulted in single amino acid substitutions of R169W, R352W, and G376D in the affected PC molecules. These abnormal PC molecules were expressed in CHO-K1 cells in the presence or absence of vitamin K, and their synthesis, posttranslational modification, and secretion were studied. PC G376D was not secreted from the cells and was gradually degraded inside the cells. There was partial secretion of PC R169W and PC R352W, but most of these molecules were not secreted but were degraded intracellularly. On the basis of pulse-chase, immunofluorescence, and endo-β-*N*-acetylglucosaminidase H digestion experiments, the majority of wild-type PC molecules localize not in the Golgi apparatus but in the rough endoplasmic reticulum inside the cells. This suggests that wild-type PC molecules are secreted immediately after γ-carboxylation and modification at the Golgi apparatus. In contrast, the mutant PC molecules were retained inside the cells even after modification of oligosaccharides at the trans-Golgi apparatus, which was probably due to impaired conformation of the abnormal molecules. Data suggest that these abnormal PC molecules were not sorted to secretory vesicles in the trans-Golgi network because of conformational defects in addition to the transport defect from the rough endoplasmic reticulum to the Golgi apparatus and were degraded inside the cells, thereby resulting in a PC deficiency in the affected patients. (***Circ Res.* 2003;92:865-872.**)

Key Words: thrombosis ■ protein C deficiency ■ intracellular protein transport

The protein C (PC) system is an important regulatory mechanism of blood coagulation, without which the integrity of the vascular system is perturbed by intravascular coagulation.[1] PC, a member of the vitamin K–dependent protein family, is synthesized in the liver and is secreted into the circulation as a zymogen, analogous to the vitamin K–dependent coagulation factors.[1–3] PC degrades the cofactors of blood coagulation, factors Va and VIIIa, on activation to activated PC by thrombomodulin-bound thrombin.[1] Human PC is synthesized as a 461-amino-acid single polypeptide chain that undergoes cotranslational and posttranslational modification, including glycosylation, γ-carboxylation, β-hydroxylation, propeptide cleavage, and conversion to the two-chain form.[1,4,5] Human PC has four N-linked glycosylation sites, three of which are located in the heavy chain.[4,6] Glycosylation at the light chain site is shown to be required for efficient secretion.[1,6] Specific Glu residues that reside in the NH_2-terminal region of the light chain are γ-carboxylated by vitamin K–dependent γ-carboxylase,[7–9] giving rise to this domain being designated the Gla domain. The γ-carboxylglutamic acid residues of PC are required for anticoagulant function. In the human PC, Asp71 is modified to a β-hydroxylated residue and is thought to be involved in high-affinity calcium ion binding.[10]

Many clinical reports have shown that patients with decreased circulating levels of PC develop thrombophilia,[11–15] with venous thrombosis in heterozygotes and purpura fulminans in homozygotes. A wide variety of genetic mutations can lead to PC deficiency and PC molecular abnormality.[11–15] We found genetic mutations in three patients with thrombotic episodes and decreased levels of plasma PC. In the present study, we expressed wild-type PC and PC mutants corresponding to the respective genetic abnormalities of each patient to elucidate the molecular mechanisms of the secretion of wild-type PC and impaired secretion of abnormal PC.

Original received October 9, 2002; resubmission received February 19, 2003; revised resubmission received March 17, 2003; accepted March 18, 2003.

From the Research Division of Cell and Molecular Medicine (M.N., J.M., S.M., K.O., J.K., T.S., Y.S.), Department of Biochemistry (H.E.), Cardiovascular Division of Ohmiya Medical Center (T.Y.), and Department of Orthopedics (Y.K., Y.H.), Jichi Medical School, Tochigi-Ken, Japan.

Correspondence to Jun Mimuro, MD, PhD, Research Division of Cell and Molecular Medicine, Jichi Medical School, Tochigi-Ken 329-0498, Japan. E-mail mimuro-j@jichi.ac.jp

Circulation Research is available at http://www.circresaha.org

DOI: 10.1161/01.RES.0000069020.87627.7D

Materials and Methods

Determination of Nucleotide Sequences of the Patient PC Gene

Genomic DNA was isolated from peripheral leukocytes by standard procedures as described.[16] DNA fragments spanning all the exons including the exon-intron boundaries of the PC gene were amplified by polymerase chain reaction using Pyrobest DNA polymerase (Takara Shuzo). The nucleotide sequences of the amplified DNA fragments were determined using a Big-Dye Terminator Cycle Sequencing Ready Reaction kit and DNA sequencer model ABI 310 (Applied Biosystems Inc).

Expression of Human PC in Cultured Cells

cDNA for human PC was a generous gift from Dr S. Hirosawa (Tokyo Medical and Dental University, Tokyo, Japan).[17] The human PC cDNA spanning the entire coding region was cloned downstream from the cytomegalovirus promoter of plasmid pcDNA3 (Invitrogen, Corp) in the appropriate orientation to make plasmid pcDNA/hPCWT for expression in mammalian cells. On the basis of the nucleotide sequence of the patient PC gene, pcDNA/hPCWT was subjected to site-directed mutagenesis using QuickChange (Stratagene) for construction of plasmids pcDNA/hPC R169W, pcDNA/hPC R352W, and pcDNA/hPC G376D. These constructs were used for expression of PC R169W, PC R352W, and PC G376D in mammalian cells.

Antibodies, ELISA, and Western Blotting

Monoclonal antibodies used in the present study have been described previously.[18,19] Antibodies JTC1 and JTC3 recognize the calcium ion–dependent conformation of the Gla domain of human PC.[19] Antibody JTC3 has been shown previously not to bind to PC_{Yonago}, a mutant PC with amino acid substitution R15G in the Gla domain.[16] Antibody JTC4 binds to the catalytic domain of PC, and its binding to the PC catalytic domain is decreased significantly after reduction. Antibody JTC5 binds to the activation peptide.[18] Polyclonal antibodies to human PC were purchased from DAKO Japan and labeled with biotin using *N*-hydroxysuccinimidobiotin. For ELISA, plastic microtiter plates were coated with either the polyclonal antibody or a monoclonal antibody in PBS at 4°C for 16 hours. After blocking with 5% casein in PBS was performed, microtiter plates were incubated with PC-containing samples in ELISA buffer (50 mmol/L Tris, 0.15 mol/L NaCl, 5 mmol/L $CaCl_2$, 1% casein, and 0.1% Triton X-100) at 37°C for 2 hours. Microtiter plates were washed and incubated with biotinylated polyclonal antibody, followed by streptavidin-labeled horseradish peroxidase and substrate. The half-maximum binding concentration of PC mutants to monoclonal antibody JTC4 was determined by incubation of increasing concentrations of cell extract PC with the monoclonal antibody–immobilized microtiter plates, followed by detection of monoclonal antibody–bound PCs by biotin-labeled polyclonal antibody, as described above. Western blotting analysis for human PC was performed as described previously except for detection of membrane-bound horseradish peroxidase–labeled antibody using chemiluminescence reagent ECL Plus (Amersham Pharmacia Biotech). The PC used as a standard for the ELISA and the control PC sample for the Western blotting studies were purified from human plasma as described.[20]

Expression of Recombinant PC In Vitro

CHO-K1 cells were cultivated in HAM-F12 medium in the absence of vitamin K. CHO-K1 cells (5×10^6) in 0.8 mL Dulbecco's PBS were incubated with 20 μg of pcDNA/hPCWT, pcDNA/hPC R169W, pcDNA/hPC R352W, or pcDNA/hPC G376D on ice for 15 minutes and subjected to electroporation at 300 V (25 μF) using a Gene Pulser (Bio-Rad Laboratories). To make stable cell lines that express wild-type PC and the three PC mutants, cells were cultured in the presence of Geneticin (250 μg/mL, GIBCO-Invitrogen Japan). Cloned cell lines were selected for PC expression by immunofluorescence using polyclonal antibody against PC. Mock-transfected cells, which were subjected to electroporation with pcDNA3 alone, were also established for the control. Cloned CHO-K1 cells expressing wild-type PC and mutant PC molecules were cultured in the presence or absence of vitamin K (10 μg/mL). Expression of PC in the conditioned medium and in cell extracts in PBS containing Triton X-100 (0.5%) and phenylmethylsulfonyl fluoride (1 mmol/L) was analyzed by ELISA and Western blotting.

Analysis of Posttranslational Modification and Secretion of PC and PC Mutants

Cells were cultured for 1 hour in methionine-deficient medium (GIBCO-Invitrogen Japan) containing 100 μCi/mL [^{35}S]methionine (NEN Life Science Products, Inc), washed with PBS, and then cultured in HAM-F12 supplemented with vitamin K (10 μg/mL). After various incubation periods, conditioned medium and cell extracts were prepared. To isolate ^{35}S-labeled PC molecules, conditioned medium and cell extracts were subjected to immunoprecipitation using polyclonal antibody against PC and protein A–coupled Sepharose CL-4B (Amersham Pharmacia Biotech). ^{35}S-labeled PC was analyzed by SDS-PAGE, followed by autoradiography, and was quantified using an image analyzer (BAS 2000, Fujifilm).

Cellular Localization of Wild-Type PC and PC Mutants

Cloned cells expressing wild-type PC and PC mutants were seeded on a glass-bottom dish coated with poly-L-lysine (Matsunami Glass Ind, Ltd). After a washing with the HBSS-HEPES buffer (Hanks' buffered salt solution containing 10 mmol/L HEPES, pH 7.4) was performed, the cells were incubated for 30 minutes at 4°C with 5 μmol/L BODIPY-TR ceramide (Molecular Probes, Inc), a fluorescent sphingolipid. Cells were then incubated in fresh medium at 37°C for 30 minutes more. Cells were fixed with 4% paraformaldehyde in PBS for 20 minutes and then permeabilized with 0.05% Triton X-100 in PBS for 10 minutes at room temperature. After 16 hours of incubation with 1 μg/mL rabbit anti-human PC antibody in PBS at 4°C, the cells were incubated with Alexa 488–labeled goat anti-rabbit IgG (H+L, Molecular Probes, Inc) for another 1 hour at room temperature. Cells were visualized using a confocal laser microscope system μ Radiance (Bio-Rad Laboratories) and ECLIPSE TE 300 (Nikon). The images (PC, green; Golgi apparatus, red) were merged for evaluation of localization of PC in the Golgi apparatus (yellow), and yellow areas and green areas (intracellular PC) were quantified using image analysis software (Mac Scope, version 2.5, Mitani Co).

Analysis of Glycosylation of Wild-Type PC and PC Mutants

Wild-type PC and mutant PC were isolated from the conditioned medium, and the extracts of cells were incubated with [^{35}S]methionine in the presence of vitamin K (10 μg/mL) or warfarin (1 μmol/L) using anti-PC polyclonal antibody and protein A–coupled Sepharose CL 4B as described above. [^{35}S]Methionine-labeled PC was then incubated with 0.1 U/mL endo-β-*N*-acetylglucosaminidase H (Endo H) in PBS, pH 6.0, in the presence of 0.1% SDS at 37°C for 16 hours. Samples were analyzed by SDS-PAGE, followed by autoradiography.

Results

Genetic Abnormalities of Patients With Decreased Levels of Plasma PC

Analysis of the PC genes of the three thrombophilic patients with decreased plasma levels of PC was performed. After sequencing all exons and exon-intron boundaries, we found independent heterozygous single nucleotide mutations of C to T at position 6268, C to T at position 8769, and G to A at position 8842 in the affected PC genes. These genetic mutations resulted in single amino acid substitution of R169W, R352W, and G376D of the respective PC molecule.

Concentration of PC in the Conditioned Medium of CHO-K1 Cells

	Polyclonal ELISA, ng/mL (%)	JTC1 ELISA, Percentage of Polyclonal ELISA	JTC3 ELISA, Percentage of Polyclonal ELISA
Wild type	702±5.10 (100%)	91.7±6.25	92.5±2.84
R169W	54.4±7.47 (100%)	83.3±8.44	91.1±7.96
R352W	59.1±5.33 (100%)	90.1±8.00	84.7±8.81
G376D	0	0	0

Concentrations of PC in the conditioned medium of CHO-K1 cells, which express wild-type PC, PC R169W, PC R352W, or PC G376D in the presence of vitamin K, were determined by polyclonal ELISA, JTC1 ELISA, or JTC3 ELISA as described in Materials and Methods. The amounts of PC determined by JTC1 ELISA or JTC3 ELISA were expressed as the percentages of that determined by polyclonal ELISA (mean±SD, n=4).

These genetic abnormalities were the same mutations reported previously,[13,17,21] but PC R352W and PC G376D had not been observed previously in the Japanese population. PC R169W has a molecular defect in the activation process by the thrombin/thrombomodulin complex,[21] and PC plasma levels are decreased, although the abnormal molecules are present in the circulation. Patients with mutants PC R352W and PC G376D reportedly develop a type I PC deficiency,[13,17] but the molecular basis for the impaired secretion of these abnormal molecules has not been reported.

Recognition of Recombinant PC Antigens in Cultured Cells by Monoclonal Antibodies

To elucidate molecular mechanisms of PC deficiency caused by these genetic and molecular abnormalities, stable CHO-K1 cell lines expressing wild-type PC, PC R169W, PC R352W, and PC G376D were created. Polyclonal or monoclonal anti-PC antibodies were used as capture antibodies in ELISAs to quantify PC antigen levels in conditioned media (Table) and in cell extracts (Figure 1). Comparison of the total antigen levels (polyclonal antibody) with binding by the monoclonal antibodies permits identification of PC molecules with altered conformation of the Gla domain (JTC1 and JTC3), catalytic domain (JTC4), or activation peptide region (JTC5). When CHO-K1 cells expressing PC were cultured in the presence of vitamin K, the level of wild-type PC in the conditioned media determined by JTC1 or JTC3 ELISA was similar to that determined by polyclonal ELISA (Table), suggesting that wild-type PC expressed in CHO-K1 cells was γ-carboxylated with proper Gla domain conformation and that CHO-K1 cells were suitable for studying the synthesis and secretion of γ-carboxylated proteins. The levels of PC R169W and PC R352W in the conditioned media determined by JTC1 or JTC3 ELISA were similar to the levels determined by polyclonal ELISA, again suggesting that the PC R169W and PC R352W were fully γ-carboxylated, although the absolute amounts of these PC mutants secreted into the conditioned medium were lower than those with wild-type PC.

In the cell extracts, wild-type PC was recognized similarly by the anti-PC polyclonal antibody and the JTC4 monoclonal antibody that binds to the serine proteinase domain (Figure 1C). In contrast, binding levels relative to the polyclonal antibody binding were significantly reduced when they were assayed using the JTC1 (19%) or JTC3 (2%) monoclonal antibodies, which recognize conformational epitopes in the Gla domain (Figures 1A and 1B). Western blotting analyses confirmed ELISA data (not shown). PC R169W and PC R352W antigen in the cell extracts also bound similarly to JTC4 and the anti-PC polyclonal antibodies, but binding was reduced to 10% to 15% on a JTC1 surface, and there was no binding at all to JTC3. Binding of PC G376D to JTC1 and JTC3 was similar to the other two mutant PC molecules from cell extracts. These data suggested that the majority of the wild-type PC and mutant PC in the cell extracts did not have a Gla domain conformation analogous to native PC. The

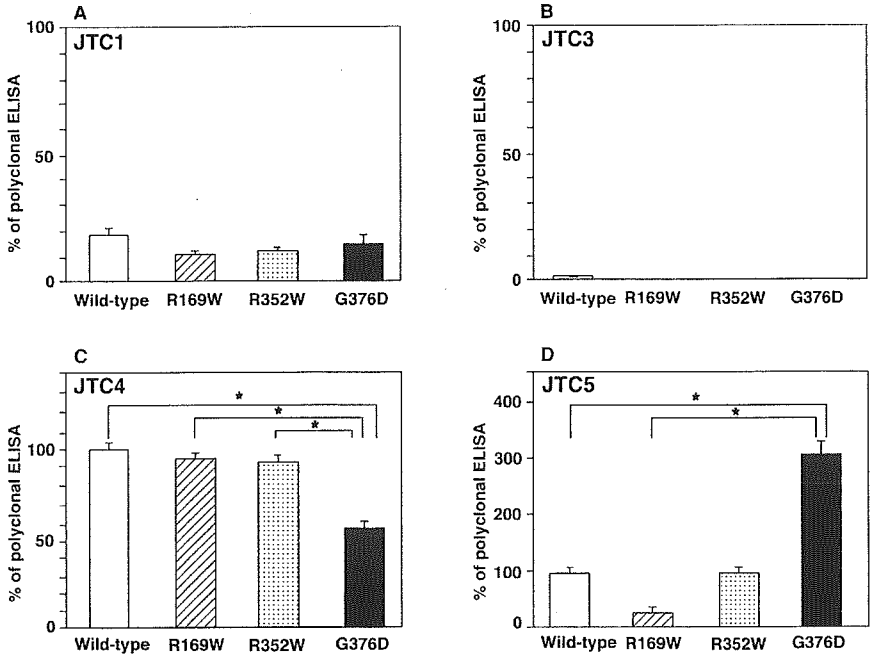

Figure 1. Analysis of recombinant PC in the cultured cells by monoclonal antibodies. Recombinant PC molecules (wild-type PC, R169W, R352W, and G376D) expressed in the cell extracts of stably transfected CHO-K1 cells were quantified by ELISA using either polyclonal antibody or monoclonal antibodies, JTC1 (A), JTC3 (B), JTC4 (C), or JTC5 (D) as a capture antibody as described in Materials and Methods. The amount of PC antigen determined using the monoclonal antibody–based assays was expressed as the percentage of that determined by the polyclonal ELISA. *$P<0.01$ (n=4).

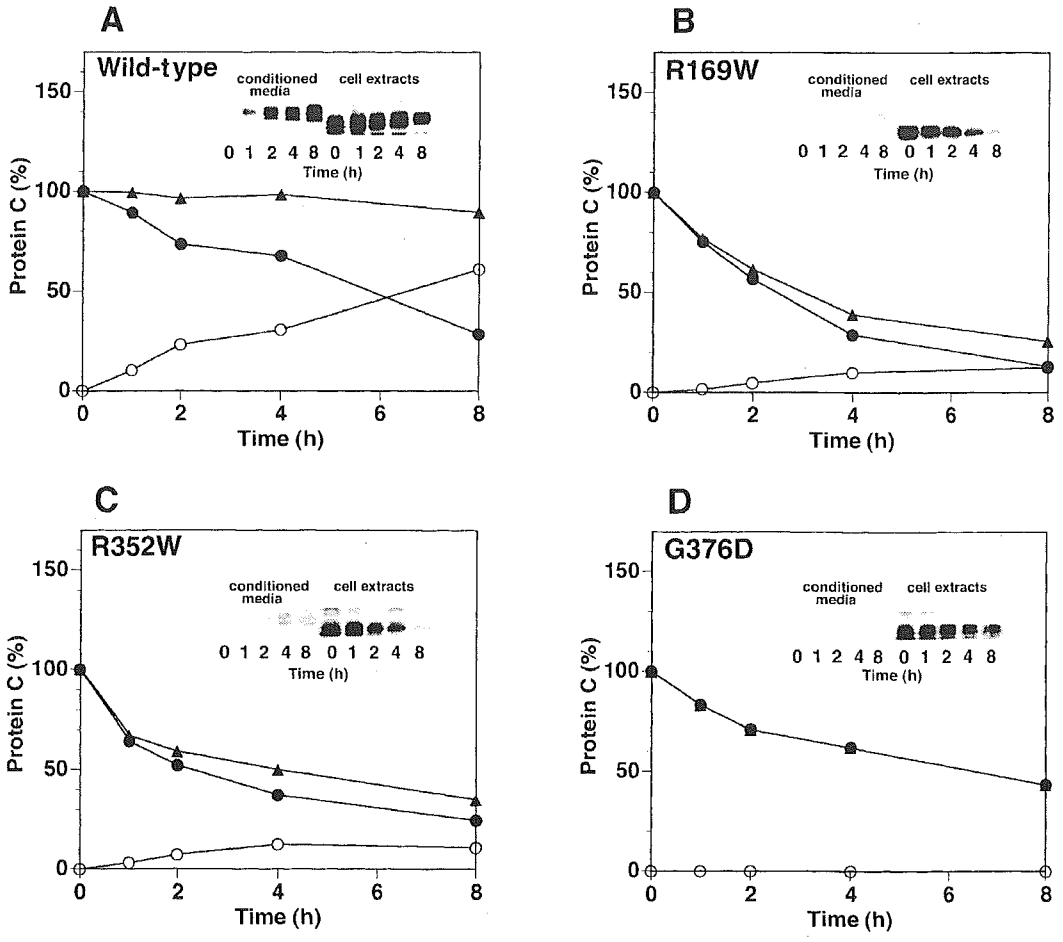

Figure 2. Analysis of synthesis and secretion of wild-type PC and PC mutants. CHO-K1 cells expressing wild-type PC (A) and mutant PC (B, R169W; C, R352W; and D, G376D) were incubated in the methionine-deficient medium in the presence of [^{35}S]methionine for 1 hour, washed, and incubated in the standard medium as described in Materials and Methods. PC molecules were isolated by immunoprecipitation and analyzed by SDS-PAGE and autoradiography (insets). After separation by SDS-PAGE, amounts of immunoprecipitated PC were quantified using an image analyzer (BAS 2000). Amounts of [^{35}S]methionine-labeled PC during chase periods were expressed as the percentages of the amount of PC after 1 hour of labeling with [^{35}S]methionine. Values are the mean of 2 independent experiments. Closed circle indicates cell extract; open circle, conditioned medium; and closed triangle, sum of PC in the cell extract and PC in the conditioned medium.

binding of PC R169W and PC R352W from cell extracts to JTC4 antibody was similar to that of wild-type PC, suggesting that the serine proteinase domain structure was relatively less affected and that the conformational changes were not global. However, binding of the PC G376D mutant from the cell extracts to JTC4 was significantly decreased relative to wild-type PC or the other mutants, indicating structural changes in the proteinase domain for this mutant. Additional observations were that the relative PC G376D concentration determined by JTC5 ELISA was ≈3-fold higher than that of wild-type PC determined by JTC5 ELISA (Figure 1D) and that the half-maximum binding of PC G376D to JTC5 was achieved at 50 ng/mL, whereas the half-maximum binding of wild-type PC to JTC5 was obtained at 230 ng/mL (not shown), suggesting that the conformational changes that occurred in the PC G376D mutant allowed JTC5 to access to the activation peptide of the PC molecule with the higher affinity. Binding of PC R352W to the JTC5 antibody was similar to that observed for wild-type PC, but binding of PC R169W was reduced ≈80%. This decrease may be accounted for by the fact that PC R169W has an amino acid substitution in the activation peptide, which probably alters the epitope for this monoclonal antibody.

Synthesis and Secretion Rates of Wild-Type PC and PC Mutants

We performed pulse-chase experiments to study the synthesis and secretion of wild-type PC and the mutants. Wild-type PC was secreted gradually from CHO-K1 cells in the presence of vitamin K during the chase period (Figure 2A). Wild-type PC in the cell extracts decreased, and the total amount of [^{35}S]methionine-labeled wild-type PC (the sum of secreted PC and the PC in the cell extracts) did not change. PC R169W and PC R352W in the cell extracts decreased faster than did wild-type PC, but only 10% of the PC molecules were secreted into the conditioned medium (Figures 2B and 2C). The total amount of [^{35}S]methionine-labeled PC decreased during the incubation period, suggesting that most of the [^{35}S]methionine-labeled PC was degraded inside the cells. PC G376D was not secreted into the conditioned medium at all,